

## Key performance indicators (KPIs): Assessing the process integration of a shell-and-tube latent heat storage unit

M. Osman<sup>a</sup>, MH. Abokersh<sup>b</sup>, O. El-Baz<sup>c</sup>, O. Sharaf<sup>d</sup>, N. Mahmoud<sup>c</sup>, M. El-Morsi<sup>a\*</sup>

<sup>a</sup> Department of Mechanical Engineering, American University in Cairo, New Cairo, Cairo, 11835, Egypt.

<sup>b</sup> Departament d'Enginyeria Mecànica, Universitat Rovira i Virgili, Av. Països Catalans 26, 43007 Tarragona, Spain.

<sup>c</sup> Department of Mechanical Power Engineering, Ain Shams University, Cairo, 11517, Egypt.

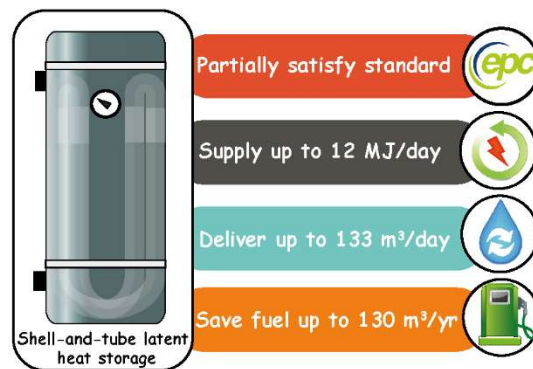
<sup>d</sup> Department of mechanical engineering, Suez Canal University, Ismailia, 41522, Egypt

\* Corresponding author: [melmorsi@aucegypt.edu](mailto:melmorsi@aucegypt.edu)

### Highlights

- A latent heat storage unit is proposed and evaluated according to a set of key performance indicators.
- Thermal energy storage unit is experimentally studied using municipal water supply.
- The multi-tube latent heat storage unit supplies hot water at a constant temperature for 3 hours.
- The proposed unit successfully recovers up to 12 MJ of thermal energy in 3 hours.
- The proposed unit saves up to 130 m<sup>3</sup> of annual natural gas consumption.

### Graphical abstract



**Keywords:** Multi-tube heat exchanger, Domestic water heating, Phase change materials, Thermal energy storage, Key performance indicators (KPI)

### Abstract

In this research, a multi-tube heat exchanger filled with phase change material (PCM) is constructed and investigated experimentally to evaluate its capability to serve as a heat storage unit in solar domestic water heating (SDWH) systems. Several operational conditions comprising the PCM initial temperature and the water discharge flowrates are included in the test as external factors to evaluate the performance of the proposed shell-and-tube latent-heat storage unit (STLHS) as a part of a SDWH system. The STLHS unit is assessed according to several quantitative, qualitative, and economic key performance indicators extracted from the Egyptian plumbing code (EPC). Firstly, the quantitative results show that the proposed STLHS unit increased the water temperature by a range of 7-12°C and maintained a constant hot water supply for extended periods, 2-3 hours. Secondly, from the qualitative point of view, the achieved heating levels are insufficient to fulfill the domestic needs according to the benchmark water temperature established by the EPC. Thirdly, evaluating the STLHS unit on an economic basis shows that the annual fuel saving increases by increasing the unit initial temperature,

where the annual fuel consumption savings reach 130 m<sup>3</sup> of natural gas. Finally, the acquired techno-economic performance measurements emphasize that the proposed unit has a notable possibility for several design modifications to achieve more improvements in its performance.

### Nomenclatures

$C_p$	specific heat [J*kg*K <sup>-1</sup> ]
D	Inner diameter [m]
$E_{user}$	energy delivered to the user [J]
$E_{heater}$	energy produced by natural gas water heater [J]
L	length [m]
$m$	mass [kg]
$\dot{m}$	mass flow rate [kg/s]
OD	outer diameter [m]
$Q_{out}$	accumulative discharged energy [J]
$\dot{Q}_{out}$	instantons thermal power [W]
$t$	time [sec]
$T$	temperature [°C]
$T_{HTF_{in}}$	water-inlet temperature [°C]
$T_{HTF_{out}}$	water-outlet temperature [°C]
$T_{norm_{user}}$	nominal user water temperature [°C]
$T_{norm_{tap}}$	average inlet-water temperature [°C]
$V_{user}$	equivalent heated volume of water served to the user [l]
$\dot{V}$	water volume flow rate [l*min <sup>-1</sup> ]
$\eta_{heater}$	efficiency of natural gas heater
$\rho$	water density [kg*m <sup>-3</sup> ]

### Abbreviations

CFD	Computational fluid dynamic
DSC	Differential scanning calorimeter
EPC	Egyptian plumbing code
FCS	Fuel consumption saving
GWH	Gas water heater
HTF	Heat transfer fluid
HX	Heat exchanger
KPI	Key performance indicators
LCOH	levelized cost of heat
LHS	Latent heat storage
LHV	Low heating value
PCM	Phase change material
SDWH	Solar domestic water heating
SHS	Sensible heat storage
STLHS	Shell-and-tube latent heat storage

## 1. Introduction

In 2015 the leaders of more than 130 countries signed the Paris climate agreement and started to apply several adaptation interventions to avoid the catastrophic consequences of the increasing levels of CO<sub>2</sub> emissions (United Nations, 2015). Moreover, the leaders established the intergovernmental panel on climate change (IPCC) and dedicated this panel to provide the scientific studies of climate change impacts and recommended policies and technological adaptations to mitigate these effects. According to IPCC special report, the energy used in the residential sector is responsible for 22% of CO<sub>2</sub> emissions worldwide (IPCC, 2018, Ma et al., 2019). A respectful part of energy consumption in the residential sector is used for water heating, where the traditional electric water heaters are responsible for 9% and 11% of energy consumption in the European Union and the United States, respectively (UNEP, 2014). Moreover, in developing countries, the primary sources for generating electric power are fossil fuels and coal, which boost the need for integrating more environmentally friendly technologies into residential energy applications. Therefore, reconstructing the energy profile of the households towards using more environmentally friendly energy sources can lead to a significant reduction in CO<sub>2</sub> emissions. Ma et al., (2019), showed that optimizing the energy structure of a Chinese house through decreasing the percentage of coal consumption by 18%, this reduction resulted in considerable mitigation for the CO<sub>2</sub> emissions from heating applications up to 68 kg CO<sub>2</sub> per household. Nevertheless, the shift towards using more environmentally friendly energy sources required different innovative solutions to tackle the randomness and lack of dispatchability of renewable energy sources. One of these solutions is effective heat management in industrial and residential sectors by using thermal energy storage (TES) (Gibb et al., 2018). The integration of TES units to the daily use of residential heating systems is essential to achieve the CO<sub>2</sub> mitigation targets. There are three different categories of TES systems which include (i) Sensible heat storage (SHS) (Li, 2016), (ii) Latent heat storage (LHS) based on phase change materials (PCMs) (de Gracia and Cabeza, 2017) and (iii) Thermochemical storage (Cot-Gores et al., 2012).

In recent years, different types of TES modules have been extensively studied in different temperature ranges and applications (Alva et al., 2018; Singh et al., 2016). Although there are several advantages and disadvantages of each TES technology, the LHS technique is remarkably considered thanks to its high energy density and isothermal charging/discharging characteristics (Zalba et al., 2003). In this context, the integration of PCM into the shell-and-tube HX exhibits a considerable advantage over other LHS methods as it combines design simplicity and reliable thermal performance (Seddegh et al., 2017b, Seddegh et al., 2017a). A significant amount of studies were dedicated to investigating the effect of the geometry design on the melting and solidification of PCM inside shell-and-tube HX as a TES unit (Han et al., 2017; Seddegh et al., 2015; Wang et al., 2016). Moreover, many researchers studied the effect of the operational parameters, such as the mass flow rate and the inlet temperature of the heat transfer fluid (HTF), on the melting/solidification cycles inside the shell-and-tube TES unit (Wang et al., 2016, Gasia et al., 2016, Gasia et al., 2017).

Most PCMs are plagued by extremely low thermal conductivity, which hinders the utilization of LHS techniques in different applications. The reported thermal conductivity of PCMs is less than 0.3 W/m-K for organic PCMs and 0.7 W/m-K for salt hydrates (Abokersh et al., 2017b; Bose and Amirham, 2016; Reddy et al., 2018). To overcome the problem of poor thermal conductivity, several solutions are proposed to increase the heat transfer surfaces such as using a finned tube (Eslamnezhad and Rahimi, 2017; Hosseini et al., 2015), or use a multi-tube HX (Agyenim et al., 2010; Jourabian et al., 2017). The researchers concluded that increasing the number of tubes remarkably enhanced the heat transfer rate and decreased the cycle time (Esapour et al., 2016; Jourabian et al., 2017). Overall, the literature shows that most of the researches leaned towards evaluating the performance of different LHS units as an isolated TES component. However, integrating the external factors from the heating system into the evaluation of the capability of these storage units to serve in domestic or industrial applications is rarely investigated.

It is challenging to design and select the suitable TES that fulfill the targets of the system requirements; this is because there are several options for integrating the TES unit into residential applications/systems. Moreover, the available energy sources, type of required energy, the available/required rate of charging/discharging are varied according to the complexity level and constraints of each system, which complicate the selection process of the appropriate TES for the target application (Gibb et al., 2018). Besides, there is a lack of a complete methodology for evaluating the TES units integrated with a thermal system, and it is indecisive to judge on the performance of an isolated TES unit without prior defining the purpose and the expected outcomes to the end-users of this unit (Giacone and Mancò, 2012; Gibb et al., 2018; Lindberg et al., 2015). Consequently, there is a necessity for a reliable evaluation of the TES units' performance based on the system requirements and the stakeholders' perspectives to determine the essential parameters and the key performance indicators (KPI) of the TES unit. Aiming at tackling the challenge associated with the TES evaluation, Gibb et al., (2018), developed a systematic methodology to evaluate the TES units where the evaluation process of any TES unit is implemented through two main steps. Firstly, the characterization of the unit's technical and economic parameters to define the performance and the constraints associated with the TES unit as an independent thermal storage module. Secondly, define the expected benefits of integrating this TES unit into the target thermal system and determine the key performance indicators (KPI) of the served process. In the proposed methodology, the TES unit should be interlinked with the thermal system where the TES performance parameters are linked and compared to the system requirements according to a set of KPI as shown in Figure 1 (Gibb et al., 2018).

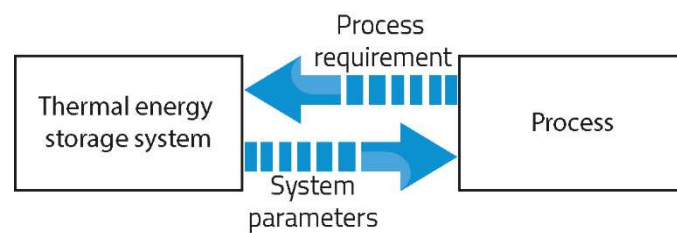


Figure 1 Linking the process requirement with the TES system parameters (Gibb et al., 2018).

Concisely, a reliable evaluation for a TES unit requires a clear specification for the storage unit, the system, and the advantages of integrating the storage unit with the thermal system according to the predefined KPIs. The KPIs of a TES unit integrated into a thermal system can be categorized as follows (Gibb et al., 2018, Cabeza et al. 2015):

1. Qualitative and quantitative indicators: evaluating a dimensionless adjective or measuring a quantity value.
2. Lagging and leading indicators: evaluating the results of a process to determine the success or failure in fulfilling the requirement.
3. Input to output indicators: evaluating the system according to its efficiency.
4. Directional indicators: evaluating the system according to its ability to be developed.
5. Financial indicators: evaluating the feasibility and the economic aspects of the system.

To the best of the authors' knowledge, the study to evaluate the performance of a TES module integrated into a solar domestic water heating (SDWH) system according to the recently proposed methodology by Gibb et al., (2018) is not fulfilled yet. Therefore, a reliable evaluation of the direct benefits for integrating an LHS module to a SDWH is still a controversial issue and requires a study that combines the unit's thermal characteristics and the unit's performance according to a pre-established set of technical and economic criteria.

Aligning with this perspective, a multi-tube LHS unit based on shell-and-tube design is introduced to be used as a retrofit within a domestic water heating system. The performance of this shell-and-tube latent heat storage (STLHS) unit within a water heating system of a single-family house is assessed according

to a set of technical and economic indicators. The novelty of this work relies on providing the non-technical end-users tangible evaluation for the performance of an LHS unit that can be used within their domestic heating system. Those end-users are considered as stakeholders whose perspective is essential to establish a reliable standard for testing the performance of LHS units. In this context, the presented experimental study examines the ability of the proposed LHS unit to fit the demand of the domestic water heating system based on reference values defined by the EPC (*MHUUC*, 1999). Accordingly, the thermal performance of the system is qualitatively and quantitatively evaluated during the discharging phase using real draw-offs conditions. Thus, municipal water as heat transfer fluid (HTF) with uncontrolled temperature and different flow rates is used, as external affecting factors, to investigate the capability of the proposed TES unit to serve as a part of a SDWH system. In addition, the outcome system performance is economically evaluated to determine the financial benefits of using this unit within the available SDWH systems.

This paper is organized as follows: section 2 presents the methodology and design criteria used to build the proposed TES unit. Section 3 presents the system design, including the experimental setup and the PCM selection criteria. Section 4 illustrates the experimental procedure and presents the list of the conducted experiments. Section 5 is dedicated to present the obtained results and discuss the key findings. Finally, section 6 presents a conclusion for the work and the several recommendations for future research.

## **2. Methodology and design criteria**

The working methodology has three main phases which are used to evaluate the performance of the proposed STLHS unit according to the presented KPI framework. Firstly, selecting the criteria that are used to design the STLHS unit and qualitatively assess its capability to serve as reliable storage in the domestic heating systems. Secondly, quantitatively assess the STLHS unit thermal performance through the inlet/outlet water temperature difference and the accumulated energy. Thirdly, the supplied hot water and the equivalent fuel saved are evaluated from a financial point of view.

### **2.1. Design criteria and qualitative analysis**

The design methodology for the TES unit of SDWH system does not depend only on the estimation of the total energy stored to ensure the functionality and the reliability of the designed system (Ahmed et al., 2016). Both the discharge flow rate and discharge phase time are essential factors that determine the capability of the system to fulfill the required domestic hot water demand (Edwards et al., 2015).

Another important aspect in designing a domestic water heating unit is the delivery temperature. The required water delivery temperature varies according to the application being served. Generally, there are two main types of hot water, tempered and un-tempered, with a delivery temperature range between 40-45°C and 55-60°C, respectively (Burch and Thorton, 2014; Fuentes et al., 2018). Tempered water is usually mixed with cold water, from the main supply, to decrease its temperature to be suitable for different applications, which include human contact such as showers, washing hands, etc. The main usage of un-tempered water is in applications with direct hot water usage such as dishwashers and washing machines.

According to the EPC (*MHUUC*, 1999), the maximum allowable water temperature that directly contacts the human skin is in the range between 54-60°C. However, for economic reasons, it is preferred to limit the water temperature range to 45-49°C. Moreover, the EPC code states that the maximum period of peak consumption is in the range between 2-3 hours during the morning hours, 6-9 am, and the evening hours, 5-8 pm. In addition, (Zhou et al., 2018) recommended that the hot water demand on the user side is 3 hours. Consequently, the performance of the proposed TES unit will be evaluated according to its ability to deliver hot water at the minimum useable temperature (45°C) during the whole peak periods (2-3 hours).

## 2.2. Quantitative analysis

In addition to the mentioned qualitative analysis, the unit will be assessed quantitatively by the amount of energy recovered during the discharge phase. The discharged energy from the TES unit is calculated using the temperature difference between the inlet and outlet temperatures of the HTF at each time step. It is assumed that the storage unit is well insulated, and the heat losses from the unit are neglected. Accordingly, the rate at which the thermal energy is discharged or released from the PCM to the water ( $\dot{Q}_{out}$ ) is calculated using Eq. (1) (Sharma et al., 2009), and (Kabbara et al., 2016).

$$\dot{Q}_{out} = \dot{m} C_p (T_{HTF_{out}} - T_{HTF_{in}}) \quad (1)$$

where  $\dot{m}$  is the HTF mass flow rate,  $C_p$  the HTF specific heat,  $T_{HTF_{in}}$  is the HTF inlet temperature, and  $T_{HTF_{out}}$  is the HTF outlet temperature. The cumulative discharged energy ( $Q_{out}$ ) is the summation of all instantaneous discharged energies over all time intervals,  $\Delta t$ , during the discharging phase, as given by Eq. (2) (Kabbara et al., 2016; Sharma et al., 2009).

$$Q_{out} = \sum_{i=0}^n \dot{m} C_p (T_{HTF_{out}} - T_{HTF_{in}}) \Delta t_i \quad (2)$$

## 2.3. Economic analysis

A reliable evaluation for the unit performance needs a normalized value to eliminate the effect of the fluctuation in water inlet temperature. Therefore, the total accumulated energy is converted to an equivalent amount of heated water supplied to the user, as given by Eq. (3) (Frazzica et al., 2016).

$$V_{user} = \frac{E_{user}}{\rho C_p (T_{norm_{user}} - T_{norm_{tap}})} \quad (3)$$

where  $E_{user}$  is the cumulative discharged energy ( $Q_{out}$ ) calculated from Eq. (2),  $V_{user}$  is the equivalent heated volume of water served to the user at the required temperature, and  $\rho$  is the water density.  $T_{norm_{user}}$  is the nominal user temperature which is fixed at 45°C as defined by EPC (MHUUC, 1999), and  $T_{norm_{tap}}$ , is the average inlet water temperature which is fixed at 20°C following the municipal plumbing code (*Egyptian Plumbing Code, Ministry of Housing, Utilities and Urban Communities, Egypt*, 1999). Furthermore, a primary economic analysis is introduced to combine the technical and financial performance of the proposed STLHS unit. In this analysis, the energy gained from the STLHS unit is compared to a conventional gas-fired water heater (GWH) with an estimated efficiency  $\eta_{heater}$  of 0.9 (Bourke et al., 2014, Park et al., 2014). Thus,  $E_{heater}$ , computed by Eq. (4) (Li et al., 2017), is used to calculate the equivalent amount of annual energy consumed by the GWH to produce the calculated  $V_{user}$ .

$$E_{heater} = \frac{E_{user}}{\eta_{heater}} \quad (4)$$

Further, the annual fuel consumption savings (FCS) are calculated to present a tangible equivalent to the volume of gas saved by using the STLHS unit to produce energy instead of the conventional GWH. The FCS can be calculated using Eq. (5) (Li et al., 2017).

$$FCS = \frac{E_{heater}}{LHV} \quad (5)$$

where LHV is the average low heating value of natural gas, which is equal to 10.5 kWh<sub>th</sub>·m<sup>-3</sup> (Li et al., 2017; Mostafavi Tehrani et al., 2013a, 2013b).

## 2.4. Uncertainty analysis

The level of uncertainty in the experimental results depends on the accuracy of the measurement tools used in this experiment. The accuracy of the measurement equipment is calculated by the manufacturer. The uncertainty of the calculated values is determined by the following equations (Rahimi et al., 2019):

$$\frac{\partial f}{f} = \left[ \left( n_1 \frac{\partial x_1}{x_1} \right)^2 + \left( n_2 \frac{\partial x_2}{x_2} \right)^2 + \dots + \left( n_n \frac{\partial x_n}{x_n} \right)^2 \right]^{1/2} \quad (6)$$

Accordingly, the uncertainty of the calculated energy discharge rate is

$$Q_{out} = f(\dot{\Psi}, T_{HTF_{out}}, T_{HTF_{in}}) \quad (7)$$

$$\frac{\partial Q_{out}}{Q_{out}} = \left[ \left( \frac{\partial \dot{\Psi}}{\dot{\Psi}} \right)^2 + \left( \frac{\partial T_{HTF_{out}}}{T_{HTF_{out}}} \right)^2 + \left( \frac{\partial T_{HTF_{in}}}{\Delta T_{HTF_{in}}} \right)^2 \right]^{1/2} \quad (8)$$

where the numerators are the uncertainty of measurement tools, and the denominators are the maximum measured values.

## 3. System design

In this experimental work, a multi-tube heat exchanger unit filled with paraffin wax is utilized as a LHS unit for SDWH system. Figure 2 shows the integration of the proposed LHS unit within the SDWH system. The STLHS unit specifications and the properties of the used PCM material will be discussed in detail in the following sections.

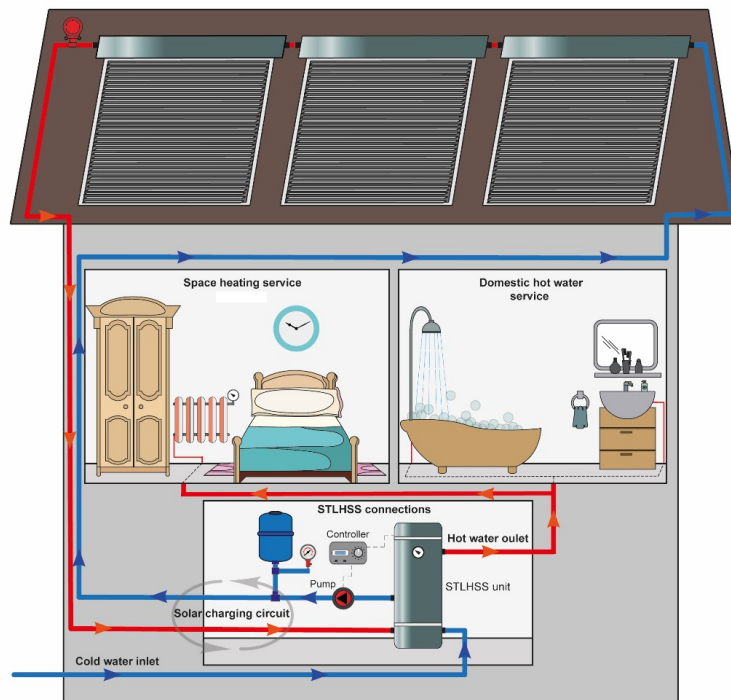


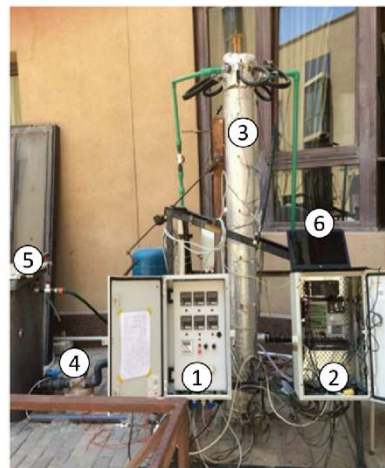
Figure 2: The proposed SDWH system with the STLHS unit arrangement

### 3.1. Experimental setup

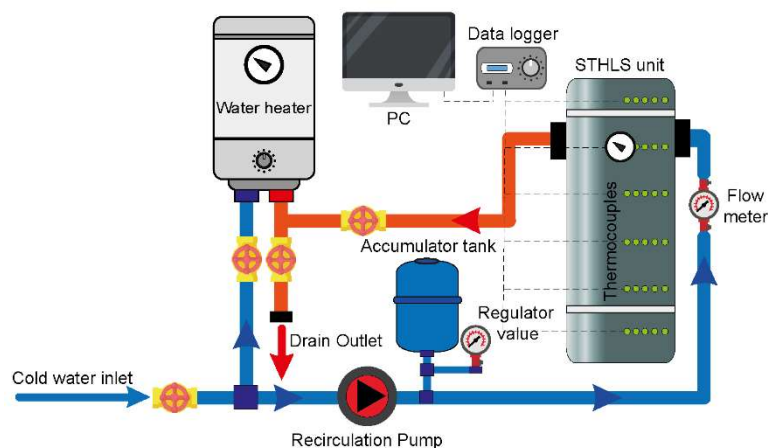
The experimental setup consists of 3 main parts, the TES tank, the water supply system, and the measurement system. The TES tank, the primary concern of the study, is a shell-and-tube HX. The shell-side is filled with paraffin wax. The water supply system is used to supply and circulate the HTF in the tube-side. While the measuring system helps in quantifying the system performance. Figure 3 shows the experimental setup for the proposed system.

The TES tank is made of a circular 2 mm thick steel pipe. The pipe is 100 mm inner diameter (D) and 1.8 m long (L). The TES tank is insulated with 45 mm layer of Rockwool with thermal conductivity  $0.035 \text{ W}\cdot\text{m}^{-1}\cdot\text{K}^{-1}$ , and the unit held vertically on a steel stand. A bundle of copper U-tubes is inserted in the TES tank vertically. The bundle consists of six U-tubes 6.3 mm outside diameter (OD) and 0.4 mm thick. The tubes are connected in series, and the intermediate temperatures are measured using six J-type thermocouples. The U-tubes are supported in place using 4 Corian rings at distances 11, 55, 55, and 43 cm from one end of the TES tank, as shown in Figure 4.

During the charging process, a domestic electric water heater with a capacity of 1500 W and a volumetric tank capacity of 80 liters is connected to a 1 HP centrifugal pump to charge the PCM. On the other hand, during the discharging process, water from mains, at ambient temperature, is pumped through the U-tubes of the HX using the same pump.



(a)



(b)

Figure 3: (a) Photograph of the STLHS unit used in the experiment, (1) temperature control, (2) Datalogger, (3) PCM unit, (4) circulating pump, (5) water storage tank, (b) schematic diagram for the experimental setup

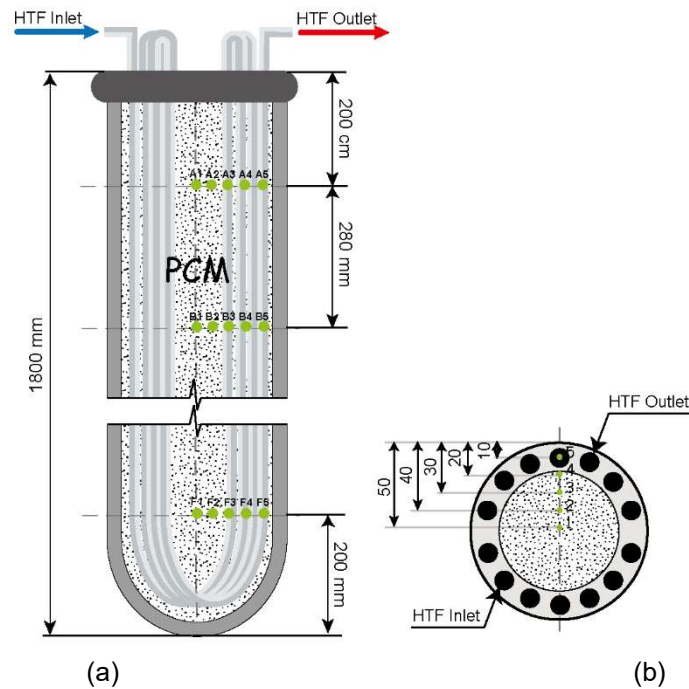


Figure 4: Schematic diagram for the STLHS system, (a) longitudinal section showing thermocouples distribution, (b) top section showing tubes connections

The PCM temperature is measured using 30 J-type thermocouples, with an accuracy of  $\pm 2.2^{\circ}\text{C}$  (OMEGA Engineering, Inc., 2016). All thermocouples used in this research are calibrated against a thermometer whose calibration is traceable to NIST and DAkkS, with an accuracy of  $\pm 1^{\circ}\text{C}$  (OMEGA Engineering, Inc., 2005). The thermocouples, grouped into six groups (A: F), are installed along the tube axial direction at distances of 20, 48, 76, 104, 132 and 160 cm from one end of the steel tube, as shown in Figure 4-a. The five thermocouples of each group are installed at a radial distance of 10, 20, 30, 40, and 50 mm measured from the inner surface of the tube, as shown in Figure 4-b. In addition, two thermocouples are used to measure the temperatures of the HTF at inlet and outlet. The thermocouples are connected to a multiplexer connected to a data logger that saves the data every 6 seconds. Finally, a rotameter with an accuracy of  $\pm 2\%$  full-scale accuracy used to measure the volume flow rate ( $\dot{V}$ ) of the HTF (OMEGA Engineering, Inc., 2009).

### 3.2. PCM selection

The selection of suitable PCM for TES unit depends on the application temperature (M.H. Abokersh et al., 2017). It should have a high latent heat of fusion, high thermal conductivity, low volume, and density changes during phase change, no sub-cooling effects during solidification, high density, and high specific heat (Kapsalis and Karamanis, 2016; Regin et al., 2008). Also, it should be chemically stable, non-flammable, and non-toxic. The availability and reasonable price are also critical factors when choosing the PCM. Based on these criteria, a commercial-grade paraffin wax, type Alex PW600, with oil content 2-3% is selected as the most suitable option (Alex wax 600, Alexandria Wax Company, Semouha Alexandria-Egypt). A pre-characterization for the thermophysical properties of the paraffin wax is recommended since it might vary according to the manufacturer (Murray and Groulx, 2014). Generally, the PCMs are characterized by calorimetric experiments like Differential Scanning Calorimeter (DSC) to obtain the enthalpy, specific heat, melting, and solidification temperatures. The characterization experiments are performed using a DSC (TA Instruments, Inc., 2016), in the Department of Chemical Engineering at King Fahd University of Petroleum and Minerals. A 6 mg

paraffin wax sample is heated from 20°C to 90°C at a rate of 5°C/min. Figure 5 shows the DSC results for the melting and solidification curves of the examined specimen. The curves illustrate that the melting and solidification temperatures are 61.8°C and 58.3°C, respectively. Other paraffin wax properties are provided by the manufacturer (Alex wax 600, Alexandria Wax Company, Semouha Alexandria-Egypt). Table 1 summarizes the thermo-physical properties of the used paraffin wax.

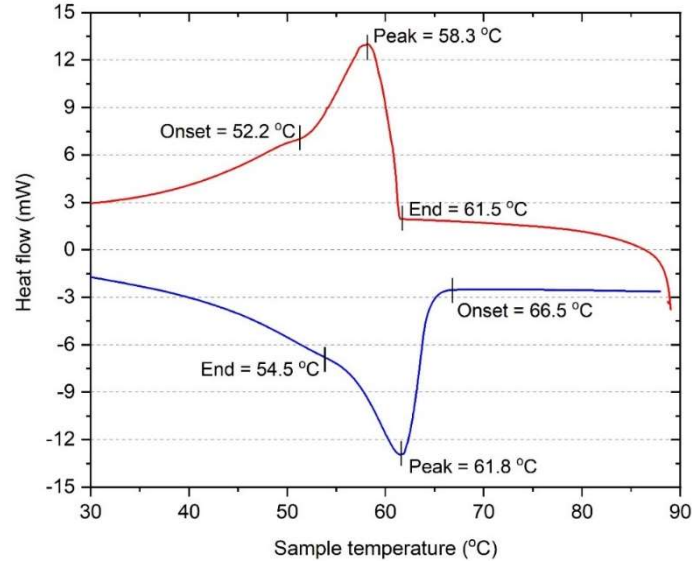


Figure 5: DSC curves of paraffin wax for melting and solidification

Table 1: Thermophysical properties of the used paraffin wax (Alex PW600)

Melting temperature	61.8°C
Solidification temperature	58.3°C
Latent heat of solidification	201.8 kJ*kg <sup>-1</sup>
Latent heat of melting	189.8 kJ*kg <sup>-1</sup>
Density (solid)	0.902 g*ml <sup>-1</sup> at 22.2°C
Specific heat capacity @25°C	1.8 kJ*kg <sup>-1</sup> *K <sup>-1</sup>

#### 4. Experimental procedure

The proposed storage unit is mainly designed to replace a conventional TES water tank in the SDWH system. Most of these systems use a control unit to maintain the hot water stored in the tank at a certain temperature. Similarly, in the proposed system, the PCM is charged to a certain temperature at the beginning of each experiment. Hot water at constant temperature is circulated through the proposed system until the PCM in the STLHS unit becomes entirely homogenous. The charging phase stops when two criteria are achieved: (i) The differences in temperature between the upper and lower PCM zones is  $\pm 2$  K, and (ii) The temperature difference between  $T_{HTF_{in}}$ , and  $T_{HTF_o}$  is  $\pm 1$  K for at least 15 min. The discharge experiments start immediately after completing the charging phase, where municipal water with un-controlled temperature is circulated through the system for 2-3 hours according to the experimental plan.

The experimental plan is designed to investigate the thermal energy discharging process under different HTF volume flow rates and initial PCM temperatures. The initial PCM temperatures are selected to examine the behavior of the LHS unit in the solid, mushy, and liquid phases. Specifically, initial PCM temperatures, 50°C, 60°C, 70°C, and 80°C, are studied to select the charging temperature that will fulfill the design criteria. Moreover, each initial temperature is examined under four different HTF discharge volume flow rates 1, 1.5, 2, 2.5, and 3 l/min. Based on the initial PCM temperature ( $T_{PCM_i}$ ), the discharge experiments are classified into four groups, as summarized in Table 2.

Table 2: Experiments plan

Group	PCM initial temperature (state)	Discharge flow rate ( $l \cdot \text{min}^{-1}$ )	Experiment number
1	50°C (solid)	1.0	1.1
		1.5	1.2
		2.0	1.3
		2.5	1.4
		3.0	1.5
2	60°C (Mushy)	1.0	2.1
		1.5	2.2
		2.0	2.3
		2.5	2.4
		3.0	2.5
3	70°C (liquid)	1.0	3.1
		1.5	3.2
		2.0	3.3
		2.5	3.4
		3.0	3.5
4	80°C (liquid)	1.0	4.1
		1.5	4.2
		2.0	4.3
		2.5	4.4
		3.0	4.5

## 5. Results and discussion

The experimental results are grouped into two main sub-sections to evaluate the outcomes of the tested units according to the established performance indicators. Firstly, the STLHS is quantitatively and qualitatively evaluated in the three different phases; solid, mushy, and liquid. The water inlet and outlet temperatures measurements are used to calculate the accumulated recovered energy ( $Q_{out}$ ). Moreover, the outlet water temperatures are used to assess qualitatively the viability of the STLHS unit to be used as a reliable TES unit within a SDWH system. Meanwhile, the PCM temperature measurements are used to detect the PCM temperature distribution along the unit to analyze the dominating heat transfer mechanism during the discharging phase. Secondly, the proposed unit is assessed on an economic basis by quantifying the annual fuel savings obtained by integrating the unit within the domestic heating system.

### 5.1 Quantitative and qualitative assessment

#### 5.1.1. Evaluate the system performance in the solid phase

This set of thermal energy discharge experiments starts when the PCM is in the solid phase, the main heat transfer mechanism is conduction, and the PCM acts as a SHS medium. Figure 6 (a) shows a sample for the instantaneous PCM average temperatures at positions A, B, C, D, E & F inside the tank and the water inlet/outlet temperatures during the thermal energy discharging experiment (1.1). The figure shows that at the beginning of the experiments the PCM temperature drops at a rate of 0.2°C/min which then decreases, and the temperature curves becomes flat. This is due to the fact that the rate of thermal energy transfer from the PCM to the water is proportional to the temperature difference ( $\Delta T$ ) between the PCM and water, which is higher at the beginning of the experiment. Also, the figure shows that the upper zone of the PCM cools before the lower zone, as it is subjected to the largest  $\Delta T$ , since the cold water enters from the top. Figure 6 (a) shows that the proposed storage unit increases the

water temperature by 5-7°C and maintains this temperature constant for about 120 min. However, the maximum water temperature reached is far below the useable temperature, 45°C. The same observation is noticed at the other water flow rates, as shown in Figure 7 (a). Accordingly, these sets of experiments were stopped after 120 min instead of 180 min. Recalling that increasing the HTF flow rate during the energy discharge phase effectively enhances the heat transfer rate and increases the total energy recovered from the TES units (Tao and He, 2011; Wang et al., 2013; Zhang et al., 2016). This set of experiments shows that this conclusion is not valid in all cases. Contrary to what is expected, Figure 8 (a) shows that the energy recovered in experiment (1.5), with the highest water flow rate ( $\dot{\psi}=3$  l/min, and  $T_{HTF_{in}}=28^{\circ}\text{C}$ ), is not the maximum. Meanwhile, the maximum energy recovered is from experiment (1.3), with the lowest inlet temperature ( $T_{HTF_{in}}=20^{\circ}\text{C}$  and  $\dot{\psi}=2$  l/min). The cumulative discharged energy from experiment (1.3) is  $9.1 \pm 1.3$  MJ, which is 21% higher than the total energy discharged from experiment (1.5). This is mainly because that the HTF inlet temperature has a significant influence on the rate of heat transfer between the PCM and the HTF. The enhancement of heat transfer between the PCM and the circulated HTF increased the discharging power and consequently increased the accumulated energy at the end of the 3 hours test.

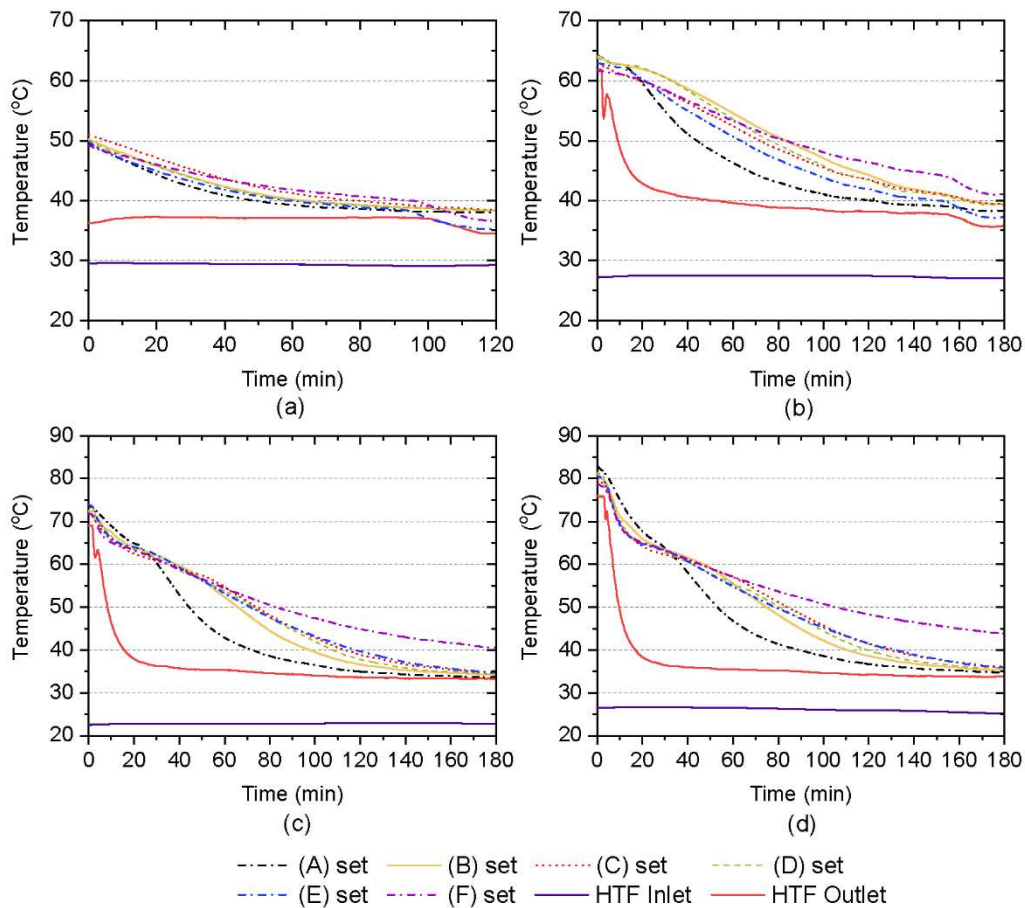


Figure 6: Temperature profile of PCM during experimental tests of a group (1) where  
(a) PCM temperatures at  $T_{PCM_i}=50^{\circ}\text{C}$ ,  $\dot{\psi}=1\text{ l}\cdot\text{min}^{-1}$ , and  $T_{HTF_{in}}=30^{\circ}\text{C}$   
(b) PCM temperatures at  $T_{PCM_i}=60^{\circ}\text{C}$ ,  $\dot{\psi}=1\text{ l}\cdot\text{min}^{-1}$ , and  $T_{HTF_{in}}=26^{\circ}\text{C}$   
(c) PCM temperatures at  $T_{PCM_i}=70^{\circ}\text{C}$ ,  $\dot{\psi}=1\text{ l}\cdot\text{min}^{-1}$ , and  $T_{HTF_{in}}=22^{\circ}\text{C}$   
(d) PCM temperatures at  $T_{PCM_i}=80^{\circ}\text{C}$ ,  $\dot{\psi}=1\text{ l}\cdot\text{min}^{-1}$ , and  $T_{HTF_{in}}=25^{\circ}\text{C}$

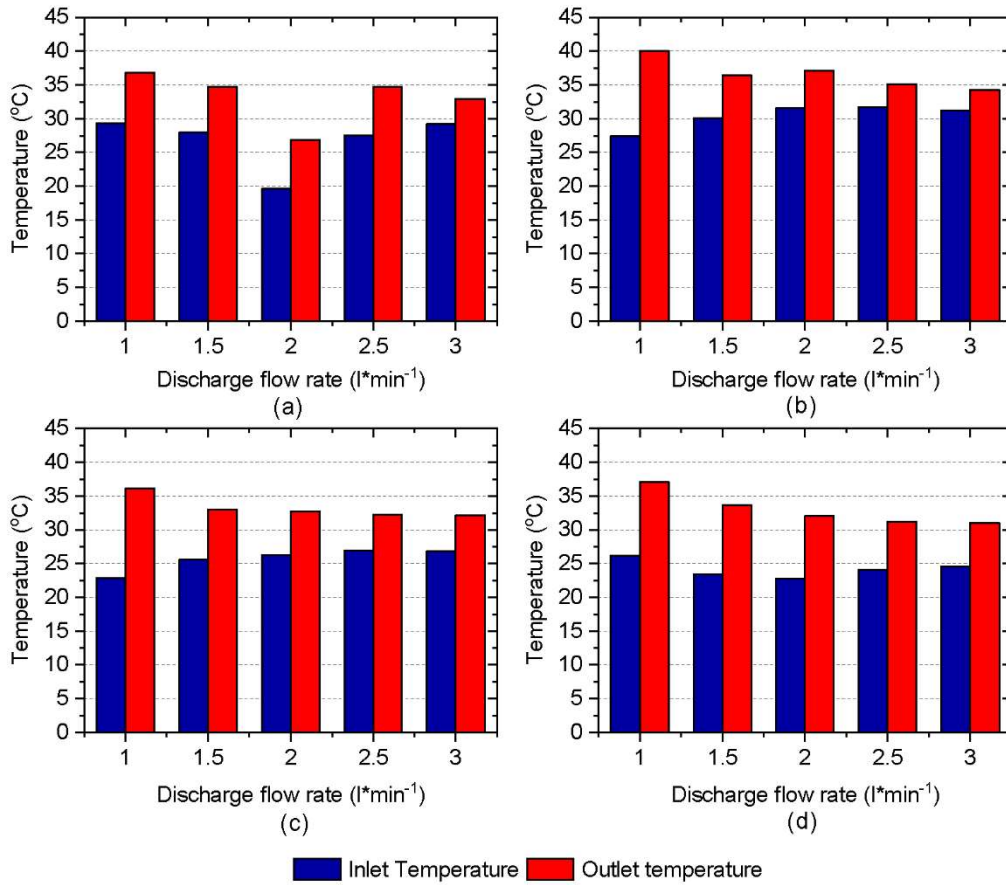


Figure 7: (a) Average water inlet and outlet temperatures for experiment group 1  
 (b) Average water inlet and outlet temperatures for experiment group 2  
 (c) Average water inlet and outlet temperatures for experiment group 3  
 (d) Average water inlet and outlet temperatures for experiment group 4

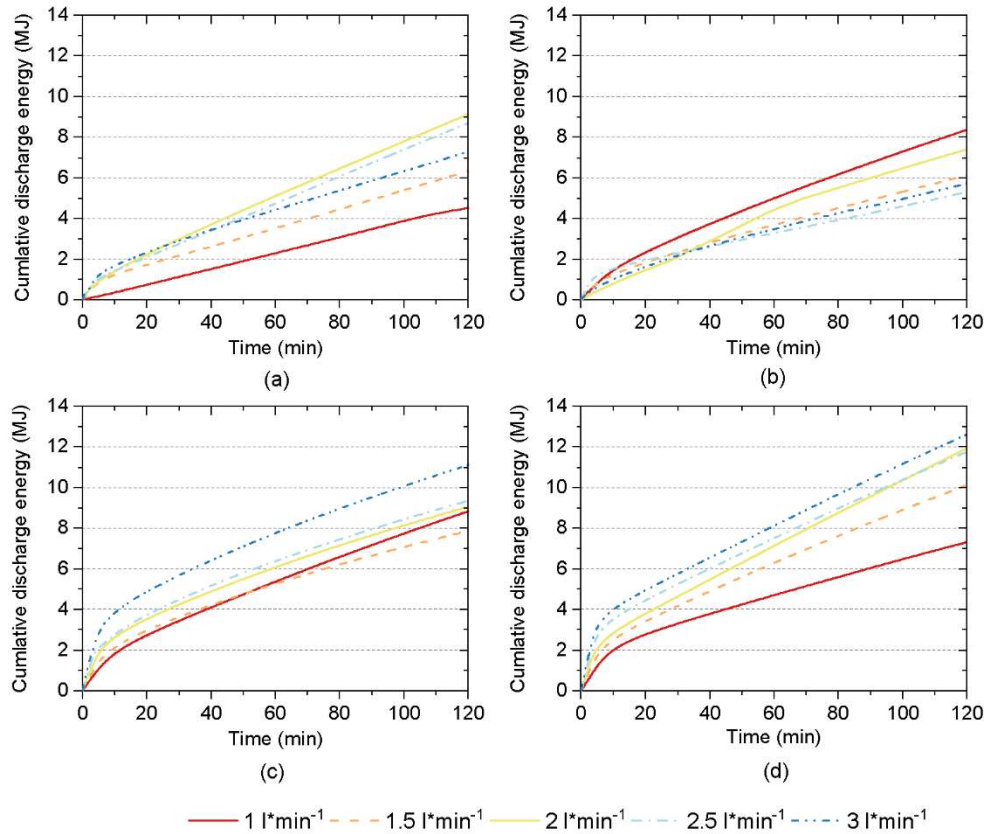


Figure 8: (a) Cumulative energy recovered during experiment group 1  
(b) Cumulative energy recovered during experiment group 2  
(c) Cumulative energy recovered during experiment group 3  
(d) Cumulative energy recovered during experiment group 4

### 5.1.2. Evaluate the system performance in the phase change region

In this set of experiments, the PCM is charged to 60°C to study the effect of increasing the PCM initial temperature on the ability of the storage unit to heat the water to the required useable temperature. Figure 6 (b) shows the instantaneous average PCM temperatures at positions A, B, C, D, E, & F during the thermal energy discharging experiment (2.1). The figure shows that the PCM temperature is almost constant at the beginning of the experiments as the PCM solidifies. The PCM temperature drops at a very slow rate of 0.11°C/min due to the phase change.

The figure shows that the water outlet temperature remains above 35°C for more than 180 min. The results show that the TES unit increases the water temperature by 5-14°C as shown in figure Figure 7:. However, the water outlet temperature is still below the required temperature, 45°C. These results indicate that the proposed TES unit partially fulfilled the vital performance benchmarks.

Figure 8 (b) shows the instantaneous cumulative discharged energy for experiments group 2. The figure shows that the maximum cumulative discharged energy is  $9.5 \pm 1.4$  MJ which is obtained from experiment (2.1), with water flow rate  $\dot{V}= 1$  l/min. While, the cumulative discharged energy obtained from experiment (2.5), with water flow rate  $\dot{V}= 3$  l/min, is  $6.8 \pm 1.5$  MJ, which is lower by 28%. This is mainly because the average HTF inlet temperature in experiment (2.1) was equal 26.8°C which is lower than the average inlet temperature in experiment 2.5 which is equal to 31°C. This increase in temperature difference between the PCM and the circulated HTF enhanced the energy recovery rate which consequently increased the accumulated energy recovered at the end of the test. These results

confirm the main finding of the previous tests that both HTF inlet temperature and flow rate should be adjusted concurrently to achieve the optimum energy recovery from the TES units.

The effect of using the multi-tube design on the homogeneity of the PCM temperature is examined using the temperature contours drawn by contouring and surface mapping software, Surfer 14, (Golden Software, LLC., 2017). The results obtained from experiment group 1 are depicted in Figure 9. The contours show the PCM temperature change as time progresses during the discharging process. For the investigated volume flow rates, the figure shows that the PCM temperature is almost uniform along the storage unit. This observation is mainly due to the recirculation of hot water from top to bottom in the TES tank, which helps to homogenates the PCM temperature along the unit.

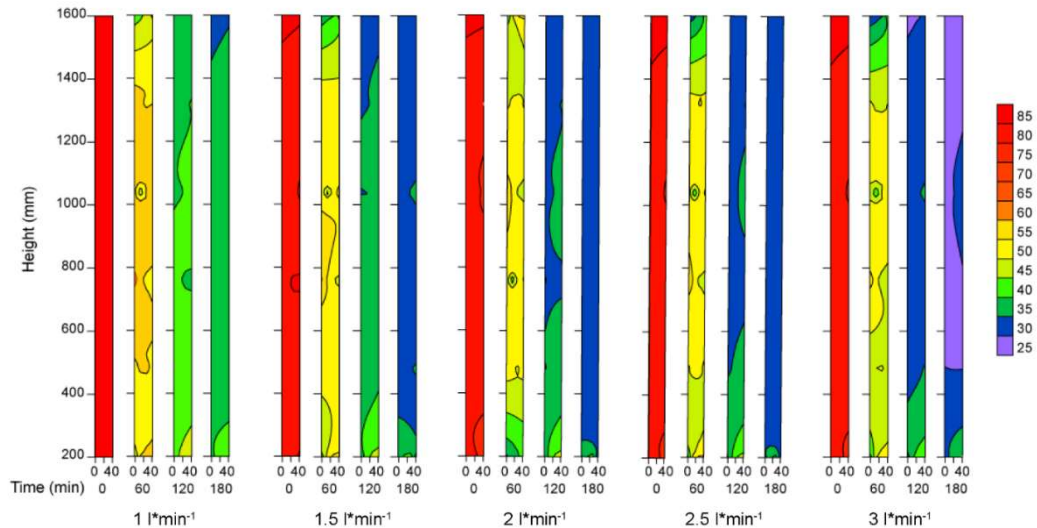


Figure 9: Temperature contours inside the storage tank at  $T_{HTF_{in}} = 60^{\circ}\text{C}$

### 5.1.3. Evaluate the system performance in the molten phase

Based on the experimental plan, a new set of experiments, groups 3 and 4, are conducted where the discharging process starts from higher initial PCM temperatures,  $70^{\circ}\text{C}$  and  $80^{\circ}\text{C}$ . These temperatures are above the phase change temperature,  $62^{\circ}\text{C}$ , by  $8^{\circ}\text{C}$  and  $18^{\circ}\text{C}$ , respectively. Figure 6 (c) and (d) show that, for an initial PCM temperature of  $70^{\circ}\text{C}$  and  $80^{\circ}\text{C}$ , the PCM temperature drops at a rate at of  $0.7^{\circ}\text{C}/\text{min}$  and  $1^{\circ}\text{C}/\text{min}$ , respectively. This is due to the high temperature difference between the HTF and the PCM and the convection currents in the molten PCM, which enhances the heat transfer. Since the dominating mode of heat transfer is convection the PCM temperature drops at rates that are 3.5-5 times higher than that for an initial PCM temperature of  $50^{\circ}\text{C}$ , where conduction is the only mode of heat transfer.

The analysis of the results of these sets of experiments show an almost similar pattern, as shown in figures 6, 7, and 8 (c and d). Hence, to avoid redundancy, only the results of experiments group 4 will be discussed after this.

The discharging experiments start while the PCM is in its molten phase. In this case, the PCM acts as a SHS unit, and natural convection are the main heat transfer mechanism. This is also the case in the mushy region. The stored thermal energy is discharged until the temperature reaches the lower solidification temperature  $58^{\circ}\text{C}$ , where conduction becomes the only mode of heat transfer between the PCM and water. Figure 6 (d) shows a sample of the instantaneous PCM average temperatures at the five different elevations inside the TES tank and the water inlet/outlet temperatures during the thermal energy discharging experiment. The results show that the unit increases the water temperature by  $6\text{-}14^{\circ}\text{C}$  and is able to maintain a hot water supply for more than 180 min. However, even at a PCM initial temperature of  $80^{\circ}\text{C}$  the TES unit is not able to increase the water temperature to the required

temperature 45°C, as shown in Figure 7 (d). In terms of the cumulative discharged energy, Figure 8 (d) shows that increasing the water volume flow rate to  $\dot{V}= 3$  l/min significantly increases the cumulative discharged energy to reach  $12.3 \pm 1.8$  MJ for experiment (4.5). This is mainly because of the low inlet water temperature during this experiment.

Although natural convection is the dominating heat transfer mechanism during the solidification of the molten PCM, the temperature contours depicted in Figure 10 illustrate that the temperature of the upper region decreases much faster than the lower levels. This observation emphasizes that the circulation of water inside the TES unit reduces the buoyancy driven convection. The cold-water inlet from the top decreases the temperature of this region much faster than the lower levels.

Finally, Figure 11 depicts the average PCM temperature at different elevations for experiments group (4), at  $t = 180$  min. The figure shows that the PCM temperature of the lowest region is higher than the other regions of the storage unit.

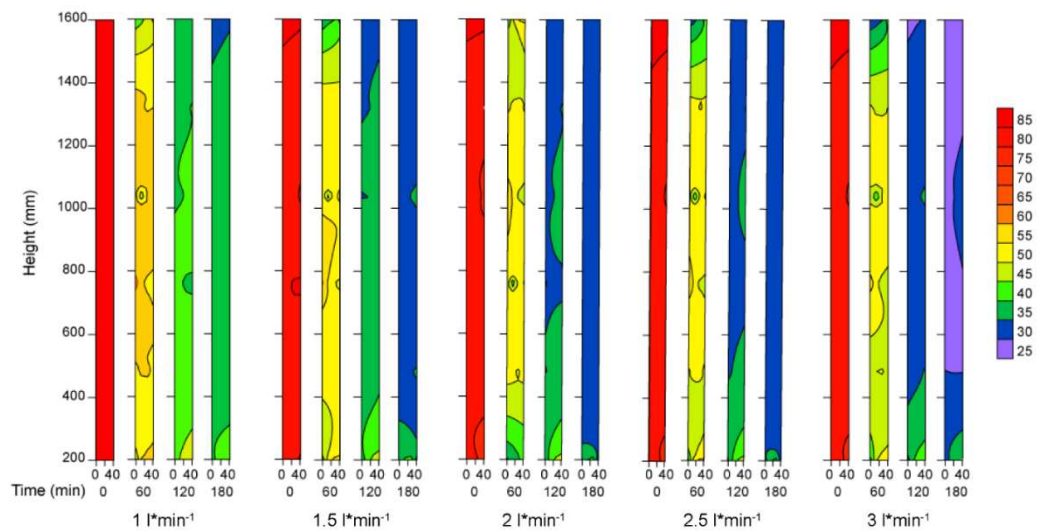


Figure 10: Temperature contours inside the storage tank at  $T_{HTF_{in}} = 80^{\circ}\text{C}$

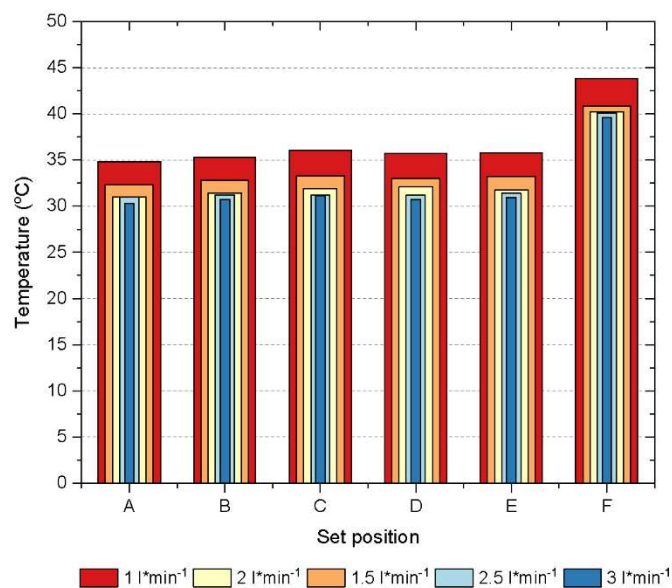


Figure 11: PCM average temperatures at different elevations for experiment group 4 at  $t=180$  min

## 5.2. Economic assessment

The average hot-water demand for a single-family house is equal to 188 l/day (MHUUC, 1999). The equivalent amount of heated water delivered to the end-user  $V_{user}$  is used to normalize the amount of hot water supplied and eliminate the effect of temperature fluctuation. As shown in Figure 12, the results confirm that the equivalent heated water from the proposed STLHS unit can cover 16% to 73% of the daily hot-water needs in the worst and best-case scenarios, respectively.

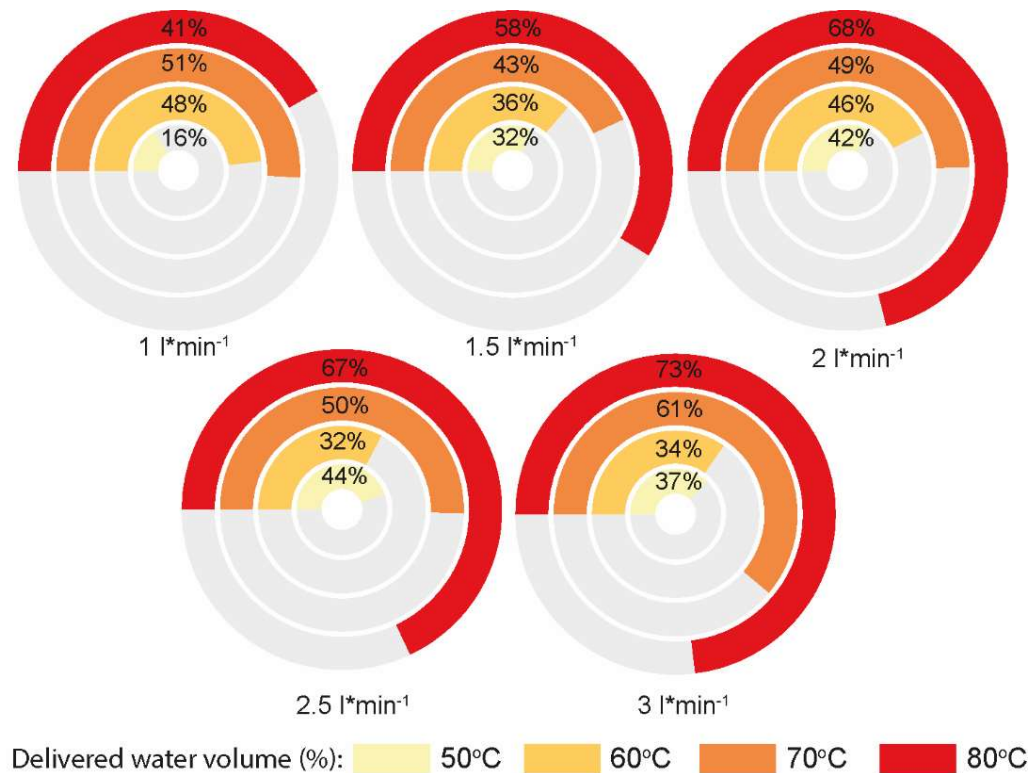


Figure 12 Equivalent water delivered to the end-user under different test conditions with 188 l/day as a daily demand.

The annual FCS is calculated to quantify the direct financial benefits of using the proposed STLHS in SDWH systems. Moreover, the FCS has quantifiable environmental benefits in addition to its economic advantages. Where, the FCS has a direct relation to the cut of CO<sub>2</sub> emissions, which is equal to 1.914 kg CO<sub>2</sub>/m<sup>3</sup> of natural gas (Tehrani et al., 2013a).

Figure 13 shows the annual savings in natural gas by using the proposed STLHS to supply the hot water needs throughout the year. The average FCS increases by 43% by increasing the initial PCM temperature from 50°C to 80°C. The annual average minimum FCS is 74 m<sup>3</sup>/year, and the average maximum is 132 m<sup>3</sup>/year. The presented primary economic analysis induces the necessity to perform more detailed techno-economic research, including financial parameters, including capital cost, maintenance expenses, fuel prices, and project lifetime. This is to optimize the STLHS unit performance and enhance its economic viability.



Figure 13 Annual fuel consumption savings with different PCM initial temperatures

## 6. Conclusion

In this research, an experimental setup is constructed to evaluate the technical and economic aspects of a TES unit based on various performance indicators in order to include different stakeholders' perspectives in the assessment process. Accordingly, a STLHS unit is used as a heat storage module for a SDHW system of a single-family house. The performance of the tested TES unit is evaluated according to a set of technical and economical KPIs extracted from the local standard. The key findings are categorized into qualitative, quantitative, and economic parameters.

- From the qualitative aspects, the proposed STLHS unit is quantitatively appraised by the accumulated energy recovered and the water temperature gradient across the unit. The analysis of the total energy recovered by using different discharge volume flow rates shows dissimilarity to the prior knowledge, and it is concluded that the effect of increasing the HTF volume flow rate on the total energy recovery is highly dependent on the HTF inlet temperature.
- From the qualitative perspective, which includes the capability of the unit to deliver hot-water at a practical temperature for a specific time frame as recommended by (Egyptian Plumbing Code, Ministry of Housing, Utilities and Urban Communities, Egypt, 1999). The results show that both the amount of thermal energy recovered, and the inlet/outlet water temperatures depend on several parameters such as the temperature difference between the inlet HTF and the PCM, HTF mass flow rate, and the specific heat of the HTF and the PCM type. Therefore, it is recommended that the HTF flow rate should be adjusted according to the application and the available HTF inlet temperature to meet the design requirements such as the discharge time duration and the useable HTF outlet temperature. Moreover, from a qualitative point of view, the proposed STLHS unit has a remarkable potential to be used as a preheater in industrial and commercial applications.
- The PCM temperature at different elevations and radial positions inside the STLHS unit is measured and analyzed. The PCM temperature contours show that the temperature of the bottom region is higher than the upper region. As such, several design parameters such as the volume-to-area ratio of the TES unit and the locations of the inlet and outlet ports need further investigation.
- From the economic perspective, the proposed unit shows a promising performance as the integration of the STLHS unit within the SDWH would save natural gas up to  $130 \text{ m}^3 \cdot \text{year}^{-1}$ . As such, the authors are planning to conduct a complete life cycle assessment to examine the techno-economic performance of the STLHS unit and compare its Levelized cost of heat (LCOH) with other TES units.
- From the stakeholders' perspective, the results obtained in this study is useful for two kinds of stakeholders. Firstly, for the end-users, comparing the performance of the proposed STLHS

unit to the standard requirements show that the proposed technology still needs further improvements to completely replace the conventional gas/electric water heaters in the current SDWH systems. However, the end-users could still benefit from this STLHS unit as a pre-heater to decrease their monthly gas bills. Secondly, for the LHS designers and manufacturers, in the light of the results obtained in this study, the energy recovery efficiency or the accumulated energy from a LHS unit only is not enough for judging the reliability of the designed module in real applications. Moreover, it is essential to ensure that the required outlet temperature is considered as the main parameter in the selection of the proper PCM for an LHS unit in a SDWH system.

Overall, this study represents the implementation of a recently developed methodology to evaluate TES units based on established KPIs. In this methodology, the influence of uncontrolled system factors are integrated within the techno-economic analysis to present a comprehensive and reliable evaluation of a thermal storage unit. Through the implementation of the proposed methodology to the STLHS unit, the results show that the unit has several tangible benefits and remarkable potential for further development. Besides, for improving the usage of the proposed TES, it is promising to develop a computational fluid dynamic (CFD) model to examine the natural circulation and the solidification of PCM within the STLHS unit during the discharging phase. This CFD model will be useful for investigating the utilization of different PCM with higher melting temperature and modify the unit configuration to determine the optimum design.

## 6. Acknowledgments

The authors would like to thank Dr. Mamdouh Ahmed Al-Harhi and Dr. Esmail M. A. Mokheimer from King Fahd University of Petroleum and Minerals for their help in evaluating the thermophysical properties of paraffin wax. Moreover, the authors would like to thank the Egyptian National Cleaner Production Center-Ministry of Trade and Industry (ENCPC-MTI), the Deutsche Gesellschaft für Internationale Zusammenarbeit (GIZ) GmbH, and Egyptian-German Private Sector Development Programme (GIZ-PSDP).

## References

- Abokersh, M.H., El-Morsi, M., Sharaf, O., Abdelrahman, W., 2017. An experimental evaluation of direct flow evacuated tube solar collector integrated with phase change material. *Energy* 139. <https://doi.org/10.1016/j.energy.2017.08.034>
- Abokersh, Mohamed Hany, Osman, M., El-Baz, O., El-Morsi, M., Sharaf, O., 2017. Review of the phase change material (PCM) usage for solar domestic water heating systems (SDWHS). *Int. J. Energy Res.* <https://doi.org/10.1002/er.3765>
- Agyenim, F., Eames, P., Smyth, M., 2010. Heat transfer enhancement in medium temperature thermal energy storage system using a multitube heat transfer array. *Renew. Energy* 35, 198–207. <https://doi.org/10.1016/j.renene.2009.03.010>
- Ahmed, K., Pylsy, P., Kurnitski, J., 2016. Hourly consumption profiles of domestic hot water for different occupant groups in dwellings. *Sol. Energy* 137, 516–530. <https://doi.org/10.1016/j.solener.2016.08.033>
- Alex wax 600, Alexandria Wax Company, Semouha Alexandria-Egypt, Telephone: +2034205210, n.d.
- Alva, G., Lin, Y., Fang, G., 2018. An overview of thermal energy storage systems. *Energy* 144, 341–378. <https://doi.org/10.1016/j.energy.2017.12.037>
- Avci, M., Yazici, M.Y., 2013. Experimental study of thermal energy storage characteristics of a paraffin in a horizontal tube-in-shell storage unit. *Energy Convers. Manag.* 73, 271–277. <https://doi.org/10.1016/j.enconman.2013.04.030>
- Bose, P., Amirtham, V.A., 2016. A review on thermal conductivity enhancement of paraffinwax as latent heat energy storage material. *Renew. Sustain. Energy Rev.* 65, 81–100. <https://doi.org/10.1016/j.rser.2016.06.071>
- Bourke, G., Bansal, P., Raine, R., 2014. Performance of gas tankless (instantaneous) water heaters under various international standards. *Appl. Energy* 131, 468–478. <https://doi.org/10.1016/j.apenergy.2014.06.008>
- Burch, J., Thorton, J., 2014. A Realistic Hot Water Draw Specification for Rating Solar Water Heaters. 2012 World Renew. Energy Forum 4–6.
- Cabeza, L.F., Galindo, E., Prieto, C., Barreneche, C., Inés Fernández, A., 2015. Key performance indicators in thermal energy storage: Survey and assessment. *Renew. Energy* 83, 820–827. <https://doi.org/10.1016/j.renene.2015.05.019>
- Cot-Gores, J., Castell, A., Cabeza, L.F., 2012. Thermochemical energy storage and conversion: A-state-of-the-art review of the experimental research under practical conditions. *Renew. Sustain. Energy Rev.* 16, 5207–5224. <https://doi.org/10.1016/j.rser.2012.04.007>
- de Gracia, A., Cabeza, L.F., 2017. Numerical simulation of a PCM packed bed system: A review. *Renew. Sustain. Energy Rev.* <https://doi.org/10.1016/j.rser.2016.09.092>
- DSC Q100, TA Instruments-Waters LLC, NewCastle, DE, United States., n.d.
- Edwards, S., Beausoleil-Morrison, I., Laperrière, A., 2015. Representative hot water draw profiles at high temporal resolution for simulating the performance of solar thermal systems. *Sol. Energy* 111, 43–52. <https://doi.org/10.1016/j.solener.2014.10.026>
- Egyptian Plumbing Code, Ministry of Housing, Utilities and Urban Communities, Egypt, 1999. . EPC 301.
- Egyptian Plumbing Code, 2005. . Ministry of Housing, Utilities and Urban Development.
- Esapour, M., Hosseini, M.J., Ranjbar, A.A., Pahamli, Y., Bahrapoury, R., 2016. Phase change in multi-tube heat exchangers. *Renew. Energy* 85, 1017–1025. <https://doi.org/10.1016/j.renene.2015.07.063>

- Eslamnezhad, H., Rahimi, A.B., 2017. Enhance heat transfer for phase-change materials in triplex tube heat exchanger with selected arrangements of fins. *Appl. Therm. Eng.* 113, 813–821. <https://doi.org/10.1016/j.applthermaleng.2016.11.067>
- Frazzica, A., Manzan, M., Sapienza, A., Freni, A., Toniato, G., Restuccia, G., 2016. Experimental testing of a hybrid sensible-latent heat storage system for domestic hot water applications. *Appl. Energy* 183, 1157–1167. <https://doi.org/10.1016/j.apenergy.2016.09.076>
- Fuentes, E., Arce, L., Salom, J., 2018. A review of domestic hot water consumption profiles for application in systems and buildings energy performance analysis. *Renew. Sustain. Energy Rev.* 81, 1530–1547. <https://doi.org/10.1016/j.rser.2017.05.229>
- Gasia, J., Diriken, J., Bourke, M., Bael, J. Van, Cabeza, L.F., 2017. Comparative study of the thermal performance of four different shell-and-tube heat exchangers used as latent heat thermal energy storage systems. <https://doi.org/10.1016/j.renene.2017.07.114>
- Gasia, J., Mir??, L., de Gracia, A., Barreneche, C., Cabeza, L.F., 2016. Experimental evaluation of a paraffin as phase change material for thermal energy storage in laboratory equipment and in a shell-and-tube heat exchanger. *Appl. Sci.* 6. <https://doi.org/10.3390/app6040112>
- Giacone, E., Mancò, S., 2012. Energy efficiency measurement in industrial processes. *Energy* 38, 331–345. <https://doi.org/10.1016/j.energy.2011.11.054>
- Gibb, D., Johnson, M., Romani, J., Gasia, J., Cabeza, L.F., Seitz, A., 2018. Process integration of thermal energy storage systems – Evaluation methodology and case studies. *Appl. Energy* 230, 750–760. <https://doi.org/10.1016/j.apenergy.2018.09.001>
- Han, G.S., Ding, H.S., Huang, Y., Tong, L.G., Ding, Y.L., 2017. A comparative study on the performances of different shell-and-tube type latent heat thermal energy storage units including the effects of natural convection. *Int. Commun. Heat Mass Transf.* 88, 228–235. <https://doi.org/10.1016/j.icheatmasstransfer.2017.09.009>
- Hosseini, M.J., Ranjbar, A.A., Rahimi, M., Bahrampoury, R., 2015. Experimental and numerical evaluation of longitudinally finned latent heat thermal storage systems. *Energy Build.* 99, 263–272. <https://doi.org/10.1016/j.enbuild.2015.04.045>
- IPCC, 2018. Summary for Policymakers.
- Jegadheeswaran, S., Pohekar, S.D., Kousksou, T., 2012. Investigations on thermal storage systems containing micron-sized conducting particles dispersed in a phase change material. *Mater Renew Sustain Energy* 1. <https://doi.org/10.1007/s40243-012-0005-7>
- Jourabian, M., Farhadi, M., Rabienataj Darzi, A.A., 2017. Accelerated melting of PCM in a multitube annulus-type thermal storage unit using lattice Boltzmann simulation. *Heat Transf. Res.* 1499–1525. <https://doi.org/10.1002/htj.21286>
- Kabbara, M., Groulx, D., Joseph, A., 2016. Experimental investigations of a latent heat energy storage unit using finned tubes. *Appl. Therm. Eng.* 101, 601–611. <https://doi.org/10.1016/j.applthermaleng.2015.12.080>
- Kapsalis, V., Karamanis, D., 2016. Solar thermal energy storage and heat pumps with phase change materials. *Appl. Therm. Eng.* 99, 1212–1224. <https://doi.org/10.1016/j.applthermaleng.2016.01.071>
- Li, G., 2016. Sensible heat thermal storage energy and exergy performance evaluations. *Renew. Sustain. Energy Rev.* 53, 897–923. <https://doi.org/10.1016/j.rser.2015.09.006>
- Li, Q., Tehrani, S.S.M., Taylor, R.A., 2017. Techno-economic analysis of a concentrating solar collector with built-in shell and tube latent heat thermal energy storage. *Energy* 121, 220–237. <https://doi.org/10.1016/j.energy.2017.01.023>

- Lindberg, C.F., Tan, S., Yan, J., Starfelt, F., 2015. Key Performance Indicators Improve Industrial Performance. *Energy Procedia* 75, 1785–1790. <https://doi.org/10.1016/j.egypro.2015.07.474>
- Ma, M., Ma, X., Cai, Weiguang, Cai, Wei, 2019. Carbon-dioxide mitigation in the residential building sector: A household scale-based assessment. *Energy Convers. Manag.* 198, 111915. <https://doi.org/10.1016/j.enconman.2019.111915>
- Mostafavi Tehrani, S.S., Saffar-Avval, M., Behboodi Kalhori, S., Mansoori, Z., Sharif, M., 2013a. Hourly energy analysis and feasibility study of employing a thermocline TES system for an integrated CHP and DH network. *Energy Convers. Manag.* 68, 281–292. <https://doi.org/10.1016/j.enconman.2013.01.020>
- Mostafavi Tehrani, S.S., Saffar-Avval, M., Mansoori, Z., Behboodi Kalhori, S., Abbassi, A., Dabir, B., Sharif, M., 2013b. Development of a CHP/DH system for the new town of Parand: An opportunity to mitigate global warming in Middle East. *Appl. Therm. Eng.* 59, 298–308. <https://doi.org/10.1016/j.applthermaleng.2013.05.016>
- Murray, R.E., Groulx, D., 2014. Experimental study of the phase change and energy characteristics inside a cylindrical latent heat energy storage system: Part 2 simultaneous charging and discharging. *Renew. Energy* 62, 571–581. <https://doi.org/10.1016/j.renene.2013.10.004>
- OMEGA Engineering, I., 2005. Omega GT-30506 Data Sheet 1–2.
- Omega FL-3663C, OMEGA Engineering, INC., Norwalk, CT -United States., n.d.
- Omega JQSS-18U-12, OMEGA Engineering, INC., Norwalk, CT -United States., n.d.
- Park, H., Nam, K.H., Jang, G.H., Kim, M.S., 2014. Performance investigation of heat pump-gas fired water heater hybrid system and its economic feasibility study. *Energy Build.* 80, 480–489. <https://doi.org/10.1016/j.enbuild.2014.05.052>
- Rahimi, M., Hosseini, M.J., Gorzin, M., 2019. Effect of helical diameter on the performance of shell and helical tube heat exchanger: An experimental approach. *Sustain. Cities Soc.* 44, 691–701. <https://doi.org/10.1016/j.scs.2018.11.002>
- Reddy, K.S., Mudgal, V., Mallick, T.K., 2018. Review of latent heat thermal energy storage for improved material stability and effective load management. *J. Energy Storage* 15, 205–227. <https://doi.org/10.1016/j.est.2017.11.005>
- Regin, A.F., Solanki, S.C., Saini, J.S., 2008. Heat transfer characteristics of thermal energy storage system using PCM capsules: A review. *Renew. Sustain. Energy Rev.* 12, 2438–2451. <https://doi.org/10.1016/j.rser.2007.06.009>
- Seddegh, S., Joybari, M.M., Wang, X., Haghghat, F., 2017a. Experimental and numerical characterization of natural convection in a vertical shell-and-tube latent thermal energy storage system. *Sustain. Cities Soc.* 35, 13–24. <https://doi.org/10.1016/j.scs.2017.07.024>
- Seddegh, S., Wang, X., Henderson, A.D., 2015. Numerical investigation of heat transfer mechanism in a vertical shell and tube latent heat energy storage system. *Appl. Therm. Eng.* 87, 698–706. <https://doi.org/10.1016/j.applthermaleng.2015.05.067>
- Seddegh, S., Wang, X., Joybari, M.M., Haghghat, F., 2017b. Investigation of the effect of geometric and operating parameters on thermal behavior of vertical shell-and-tube latent heat energy storage systems. *Energy* 137, 69–82. <https://doi.org/10.1016/j.energy.2017.07.014>
- Sharma, A., Tyagi, V. V., Chen, C.R., Buddhi, D., 2009. Review on thermal energy storage with phase change materials and applications. *Renew. Sustain. Energy Rev.* 13, 318–345. <https://doi.org/10.1016/j.rser.2007.10.005>
- Singh, R., Lazarus, I.J., Souliotis, M., 2016. Recent developments in integrated collector storage (ICS) solar water heaters: A review. *Renew. Sustain. Energy Rev.* 54, 270–298.

<https://doi.org/10.1016/j.rser.2015.10.006>

Surfer 14 Full User's Guide, Golden Software, LLC, 2017, n.d.

Tao, Y.B., He, Y.L., 2011. Numerical study on thermal energy storage performance of phase change material under non-steady-state inlet boundary. *Appl. Energy* 88, 4172–4179. <https://doi.org/10.1016/j.apenergy.2011.04.039>

UNEP, 2014. Decoupling 2: technologies, opportunities and policy options. A Report of the Working Group on Decoupling to the International Resource Panel. E.U. von Weizsäcker, J. de Lardereel, K. Hargroves, C. Hudson, M. Smith and M. Rodrigues.

United Nations, 2015. PARIS AGREEMENT.

Wang, W.W., Zhang, K., Wang, L.B., He, Y.L., 2013. Numerical study of the heat charging and discharging characteristics of a shell-and-tube phase change heat storage unit. *Appl. Therm. Eng.* 58, 542–553. <https://doi.org/10.1016/j.applthermaleng.2013.04.063>

Wang, Y., Wang, L., Xie, N., Lin, X., Chen, H., 2016. Experimental study on the melting and solidification behavior of erythritol in a vertical shell-and-tube latent heat thermal storage unit. *Int. J. Heat Mass Transf.* 99, 770–781. <https://doi.org/10.1016/j.ijheatmasstransfer.2016.03.125>

Zalba, B., Marín, J.M., Cabeza, L.F., Mehling, H., 2003. Review on thermal energy storage with phase change: materials, heat transfer analysis and applications. *Appl. Therm. Eng.* 23, 251–283.

Zhang, P., Ma, F., Xiao, X., 2016. Thermal energy storage and retrieval characteristics of a molten-salt latent heat thermal energy storage system. *Appl. Energy* 173, 255–271. <https://doi.org/10.1016/j.apenergy.2016.04.012>

Zhou, Z., Liu, J., Wang, C., Huang, X., Gao, F., Zhang, S., Yu, B., 2018. Research on the application of phase-change heat storage in centralized solar hot water system. *J. Clean. Prod.* 198, 1262–1275. <https://doi.org/10.1016/j.jclepro.2018.06.281>